HAYATI
Journal of Biosciences

Vol. 30 No. 5, September 843-854
DOI:10.4308/hjb.30.5.843-854
ISSN: 1978-3019
EISSN: 2086-4094

Antifungal Substances Produced by *B. subtilis* Strain W3.15 Inhibit the *Fusarium oxysporum* and Trigger Cellular Damage

Rury Eryna Putri[1], Nisa Rachmania Mubarik[2*], Laksmi Ambarsari[3], Aris Tri Wahyudi[2]

[1]*Study Program of Microbiology, Graduate Program, IPB University, Bogor 16680, Indonesia*
[2]*Department of Biology, Faculty of Mathematics and Natural Sciences, IPB University, Bogor 16680, Indonesia*
[3]*Department of Biochemistry, Faculty of Mathematics and Natural Sciences, IPB University, Bogor 16680, Indonesia*

ARTICLE INFO

Article history:
Received January 2, 2023
Received in revised form April 11, 2023
Accepted April 20, 2023

KEYWORDS:
biocontrol,
bacterial extract,
EA,
hyphal alteration,
malondialdehyde

ABSTRACT

Soybean *Fusarium* wilt and root rot disease caused by a necrotrophic ascomycete pathogen, *F. oxysporum*, triggered severe damage to the plant tissues and organs and impacted heavy losses. Biocontrol agents, *Bacillus subtilis*, were commonly used to produce a broad spectrum of antifungal substances and were gradually used in biocontrol studies for plant disease management. Investigation and determination of the inhibiting mechanism of antifungal substance produced by *B. subtilis* on *F. oxysporum* should be done to protect the soybean plant. This study revealed that basal nutrient broth (NB) gives the best antifungal activity. The stationary phase of the bacterial growth curve was obtained on two days of cultivation and showed the maximum antifungal activity against *F. oxysporum*. Ethyl acetate (EA) extraction of bacterial supernatant generated crude EA extract, which showed half inhibition (IC_{50}) at 306.42 µg/ml obtained from the dose-response regression curve. Post-treatment mycelia of *F. oxysporum* with bacterial extract were demonstrated as hyphal deformation followed by malondialdehyde (MDA) accumulation. Furthermore, cellular leakage on fungal cells that may be triggered by antifungal compounds from strain W3.15 occurred. Last, the related antifungal compounds were predicted to be epicatechin and benzophenone from the LC-MS/MS analysis of crude EA extract. Accordingly, the biocontrol agent *B. subtilis* strain W3.15 promises a strong potency for biofungicide development.

1. Introduction

Currently, biocontrol agents, including the related bioactive compounds product, were restrained and developed to substitute synthetic fungicides in plant disease management. The hazardous effect on a broad aspect of the environmental community and resistance character development by intensive lethal chemical application underlies the shifting in people's concern about controlling crop disease. Commonly studied biocontrol agents, the *Bacillus* group, i.e., *B. subtilis, B. mojavensis*, and *B. velezensis* (Miljaković *et al.* 2020; Saxena *et al.* 2020) were reported to produce various bioactive compounds. Those bioactive compounds were used against popular crop pathogenic fungi such as *Colletotrichum* spp., *Sclerotinia sclerotiorum, Botrytis cinerea*, and species complex *Fusarium oxysporum* (Cheung *et al.* 2020; Derbyshire *et al.* 2022; Karlsson *et al.* 2021; Wan *et al.* 2021). The cyclic lipopeptide group and several cell wall-degrading enzymes were produced by biocontrol bacteria, *B. subtilis* (Dimkić *et al.* 2022; Li *et al.* 2021). The studies on the synergism of biocontrol bacteria and their antifungal substances suggested more alternatives in plant disease biocontrol strategy.

Various destructive plant diseases reported in economic crops, such as wilt and root rot, were caused by widespread pathogenic fungi, *F. oxysporum* (Fox) (Attia *et al.* 2022; Bhagat *et al.* 2022). These soil-borne filamentous fungi were distributed worldwide and infected thousands of species of crops, i.e., wheat, tomatoes, banana, beans, and many more (Bhar *et al.* 2021; Srinivas *et al.* 2019). The *Bacillus* group, *B. subtilis*, shows strong efficacy in defeating the infection of *F. oxysporum* in crops by producing bioactive compounds. The newest report informed the potency of *B. subtilis* HSY21 as biological control

* Corresponding Author
E-mail Address: nrachmania@apps.ipb.ac.id

agent against *F. oxysporum* infection, which showed a similar response with FoERG3-knock out mutant, including deformity and swelling of the mycelium surface, increased membrane permeability, and influences the fungal virulence factor (Han *et al.* 2022). Other reports related to popular Bacilli lipopeptide showed the antimicrobial activity of *B. subtilis* (OK662659) supernatant against *F. oxysporum* f. sp. radicis-lycopersici that revealed identified as surfactins and plipastatins by LC-HRMS analysis (Munakata *et al.* 2022). Mass spectrometry such as Gas-Chromatography (GC) and Liquid Chromatography (LC) mass spectrometry (MS) with various types of additional analysis were commonly used to identify the chemical compounds related to the antifungal activity of the bacterial product.

Furthermore, one of the antifungal compounds' modes of action affected pathogens' physiological metabolism. Zhao *et al.* (2022a) found that the cell-free supernatant (CFS) generated from *B. velezensis* A4 affected the hyphal cell of postharvest grey mould, Botrytis cinerea. CFS treatment could destroy the cell membrane, resulting in exosmosis of cell contents and accumulating the reactive oxygen species (ROS) that leads to oxidative damage. The biocontrol mechanism of antifungal protein produced by *B. licheniformis* W10 revealed a destructive effect on peach shoot blight fungus, *Phomopsis amygdali*, by distorting hyphal cells, breakage the fungal cell wall and protoplasm leakage (Ji *et al.* 2022). The change of malondialdehyde (MDA), a small water-soluble molecule that is released triggered by cell membrane damage, on pathogen cells reflected an important indication of negative effects by the treatment of antifungal compounds. Intensive studies on the antifungal substances mechanism in defeating pathogenic fungi provided in-depth information for developing the bio-based fungicide to control plant disease.

In the previous research, Putri *et al.* (2021) reported the potent growth inhibition of *F. oxysporum* and hyphal alteration by cell-free supernatant (CFS) of *B. subtilis* strain W3.15. However, the fungal inhibition of that *F. oxysporum*, isolated from the soybean plant, still requires further investigation and identification of the bacterial compounds that may involve in the action. Therefore, this present study primarily focussed on producing the antifungal substances from strain W3.15 on a favorable medium and proper harvesting time. Next, the antifungal substances were explored then the evidence of *F. oxysporum* growth and microstructural deformation after treatment was determined. The effect of the antifungal substance on fungal cells using malondialdehyde level and cellular leakage were also examined. Moreover, LC-MS/MS analysis was also used to analyze and predict the chemical compound. This study provides additional information about unusual compounds type and simple mechanisms of antifungal compounds found in *B. subtilis* to inhibit *F. oxysporum.*

2. Materials and Methods

2.1. Microbial Preparation

A bacterial isolate with code W3.15 from the previous study (Putri *et al.* 2021) was used for the experiment. The strains were cultured in nutrient agar (NA, Merck, Germany) medium overnight before being examined. *F. oxysporum*, also from the previous study (Putri *et al.* 2021), was used as the phytopathogen target. The fungus was grown on potato dextrose agar (PDA, Merck, Germany) for 6 days. For conidiospore inoculum, six days old of *F. oxysporum* culture was added with an amount of 10% (v/v) Tween 80, then mixed with vortex for a few minutes. The conidiospore suspension was then transferred aseptically into 50 ml of fresh potato dextrose broth (PDB) (Difco, US). The final conidiospore concentration was counted using the total plate count (TPC) method and adjusted to 105 CFU/ml before being used in experiments.

2.2. Medium Optimization for Antifungal Compounds Production

Several types of media were used in bacterial cultivation to obtain the best growth medium for antifungal production, as described by Liu *et al.* (2015) and Sa-Uth *et al.* (2018). There was nutrient broth (NB) (Merck, Germany), trypticase soy broth (TSB) (Merck, Germany), Luria-Bertani (LB) broth (tryptone 20 g/l, yeast extract 10 g/l, NaCl 10 g/l, and distilled water), and potato dextrose broth (PDB) (Difco, US) that used. They were performed in the incubation shaker at 120 rpm for 72 h at room temperature (±28°C). Bacterial cell growth was determined by the cell biomass, whereas their antifungal activity was presented by the diameter of the inhibition zone around the paper disc after 4-5 days of incubation. This assay was conducted three times.

2.3. Correlation of Bacterial Cell Growth and Antifungal Activity

A volume of 50 ml of potato dextrose broth (PDB) (Difco, US) medium was inoculated with 1% of a fresh culture of strain W3.15 and then shaken at 120 rpm for 72 h (±28°C). During incubation, two milliliters of bacterial culture were withdrawn every three hours to measure the OD_{600} and its bioactivity with *F. oxysporum* (Li *et al.* 2018). *In vitro* evaluation of bacterial bioactivity was performed with agar disc diffusion then the inhibition zone was measured after 4-5 days of incubation in dark conditions (Hwang and Song 2020; Veras *et al.* 2016). The experiments were performed in triplicate.

2.4. Bacterial Cultivation and Extraction of Crude Antifungal Compounds

A volume of W3.15 strain seed broth was transferred into a 5 L Erlenmeyer flask containing 3 L of NB medium and incubated for two days. Culture supernatant was collected and added with ethyl acetate (EA) in equal volumes, then shaken vigorously for 24 h using a magnetic stirrer. The culture medium was removed, and the organic phase was collected and evaporated at 40°C temperature using a vacuum evaporator (Jinal and Amaresan 2020; Mohan *et al.* 2016). The crude EA extract was then stored at 4°C before being examined.

2.5. Determination of Antifungal Activity Crude EA Extract against *F. oxysporum*

The EA extract of the W3.15 strain from the previous step was diluted in several different concentrations (0-1,000 µg/ml) with 10% (v/v) of DMSO (Merck, Germany). Each concentration of the bacterial extract was added into molten PDA medium (±40°C) before being poured into a nine cm-diameter Petri dish. Negative control was chosen from the DMSO-treated plate without extract supplementation. A 5 mm of the mycelial block was cut from the six days-old *F. oxysporum* culture and then inoculated into the center of each plate. Plates were incubated under dark conditions at room temperature (±28°C) until the control plates were covered with fungal radial growth. Mycelial radial growth was used as an inhibition effects indicator compared to their respective control (Qi *et al.* 2019). The percentage of mycelial growth inhibition was calculated using the following standard equation:

$$\text{Growth inhibition percentage (\%)} = [(C - T)/C] \times 100$$

Where C was the average diameter of the control, and T was the average diameter of the fungal with extract treatment. The assay was performed in triplicates. In addition, the median inhibitory concentration (IC_{50}), defined as the concentration of crude EA extract of W3.15 strain to inhibit half of the *F. oxysporum* growth, was determined from the linear regression analysis of dose-response curve plotting between crude EA extract and mycelial average diameter (Mejri *et al.* 2018).

2.6. Light Microscopy Observation of Mycelial Morphology after Antifungal Treatment

Evaluation of mycelial growth alteration stimulated by bacterial crude extract treatment was carried out according to Li *et al.* (2021) with several modifications. Fungal mycelium was sampled from the previous treatment plates and then immersed with lactophenol blue staining before being observed under an optical microscope (Leica Microsystem, Germany) with 400x magnification. Control plates with only EA supplementation were also sampled as a comparison to normal hyphal growth.

2.7. Determination of Lipid Peroxidation Content in Fungal Mycelium

Lipid peroxidation level on extract post-treatment mycelia was expressed as malondialdehyde (MDA). *F. oxysporum* was cultured in 100 ml medium supplemented with IC_{50} concentration of crude EA extract for three days (dark condition, 25°C) before being collected using centrifugation. Mycelia (1-1.5 g) was rinsed with phosphate buffer saline (0.1 M, pH 7) and dried with filter paper. Mycelia was ground and homogenized with 5 ml of precooled 5% (w/v) trichloroacetic acid (TCA) (Merck, Germany) solution. Mycelial MDA was recovered from a homogeneous solution using centrifugation at 10,000 rpm for 10 minutes (4°C). Then, 4 ml of 0.1% (w/v) thiobarbituric acid (TBA) in 20% (w/v) TCA was added to 2 ml of the supernatant. The solution was heated in a water bath at 80°C for 15 minutes and then quickly cooled in an ice bath. Besides, sterile distilled water was used as a negative control with the same treatment (Sun *et al.* 2021). The final solution absorbance was measured using a spectrophotometer at wavelength 532 and 600 nm, respectively.

2.8. Detection of Cell Membrane Damage

Mycelia (50 mg) was harvested from three days-old *F. oxysporum* broth culture (dark condition, 110 rpm, 25°C). The collected mycelial was washed with sterile distillate water before resuspending in 20 ml of sterile distillate water supplemented with IC_{50} dosage of crude EA extract. This mixture was then incubated at room temperature (25°C, 110 rpm) for four hours with an hour (60 min) interval sampling. Afterward, the sample was filtered using a Millipore syringe filter then the supernatant was recovered and used to determine optical density at 260 nm and 280 nm to assess the nucleic acid and protein leakage. Distillates water was used as the negative control (Wang *et al.* 2020).

2.9. Secondary Metabolites Identification

LC-MS/MS system (Waters, US) analysis was used to predict the antifungal metabolites contained in crude EA extract of the W3.15 strain, as Listyorini *et al.* (2021), with certain modifications. Five microliters of crude EA extract of W3.15 strain (dissolved in methanol) were injected into an LC-MS system equipped with a UPLC capillary column C18 2.1 × 100 mm (1.8 µm) containing a column containing the Acquity UPLC®HSS 1.7 m particles. The flow rate was programmed at 0.2 ml/min at room temperature (25°C). Two types of mobile phase which consisted of a mixture of 5 mM formic acid in distilled water (A) and a mixture of 0.05% (v/v) formic acid in acetonitrile (B), were used. For mass spectrometric conditions, the electrospray ionization (ES) (Xevo G2-S Qtof) (Waters, US) system on positive ion mode was performed for further analysis. The MS/MS spectra were obtained with a mass ranging from 50–1,200 m/z. MassLynx software (ver. 4.1) was used for data acquisition and processing, and then Chemspider (www.chemspider.com) and MassBank (www.massbank.jp) were used to identify the m/z peak of the dominant spectrum.

3. Results

3.1. Effects of Different Mediums on Biomass and Antifungal Activity

Production of metabolites and biomass of the bacterial culture may increase with medium optimization. From the four types of media cultivation used to grow the strain, the TSB medium was the best medium to increase the bacterial biomass, with a yield of 9.71±0.04 g/l (w/v) (Table 1) in 72 h cultivation. Hence, the inhibition zone diameter of the 72 h-old culture supernatants from the TSB medium was only 1.85±0.03 cm, lower than the PDB medium activity with equal cultivation time. The NB medium highlighted showed the best antifungal activity from the wider diameter of the clear zone towards *F. oxysporum* colonies (2.07±0.03 cm) (Table 1). The least biomass cell and fungal inhibition activity were shown from the LB medium, with a yield of 6.72±0.31 g/l (w/v) and a diameter of inhibition at 1.62±0.01 cm, respectively. Therefore, the NB medium was used for further studies, even though the TSB medium showed the highest biomass accumulation.

3.2. Growth Correlation with the Antifungal Activity of W3.15 Strain

The W3.15 strain was cultivated under a limited environment in laboratories with its optimum cultivation medium for metabolite production. The W3.15 strain entered the logarithmic growth phase after being cultured for six h in NB medium, with almost no lag phase. Fungal growth inhibition of strain W3.15 CFS was detected at the stationary phase (12 h) with 20-30% inhibition. Then, the growth progressively prolonged to a stationary phase (>20 h) as bacterial cells rapidly growth during the logarithmic growth phase. After two days of cultivation, bacterial cell-free supernatant (CFS) showed the most potent antifungal activity against

Table 1. Effect of different basal mediums for *B. subtilis* strain W3.15 cultivation on bacterial biomass (g/l) and diameter of fungal growth inhibition (cm) during several time intervals of incubation (h). The same letter indicates no significant differences between treatments ($p<0.05$)

Media	Biomass (g/L ± SD)			Inhibition zone diameter (cm, mean ± SD)		
	24 h	48 h	72 h	24 h	48 h	72 h
TSB	2.52±0.28^{c}	5.03±0.15^{c}	9.71±0.04^{b}	1.03±0.02^{d}	1.78±0.03^{d}	1.85±0.03^{b}
LB	2.75±0.11^{c}	4.10±0.31^{a}	6.72±0.31^{a}	0.82±0.03^{b}	1.62±0.01^{a}	1.62±0.01^{a}
PDB	1.44±0.10^{a}	4.01±0.47^{a}	7.39±0.09^{c}	1.22±0.04^{e}	1.89±0.02^{e}	1.93±0.01^{c}
NB	2.19±0.54^{b}	4.64±0.08^{b}	8.34±0.01^{d}	1.50±0.01^{f}	2.07±0.03^{d}	1.99±0.02^{f}

F. oxysporum, with 50% inhibition (36 h) (Figure 1). Moreover, during 72 h cultivation, the decline phase did not appear. Still, the antifungal activity slightly declined after 36 h. It assumed that W3.13 strain growth has positively correlated with metabolite production over a two-days growth period. The strain also has an optimum harvest time in two days of cultivation for maximum antifungal activity against *F. oxysporum in vitro*.

3.3. Mycelial Growth Inhibition of Crude EA Extract from W3.15 Strain

This study investigated the effect of crude EA extract on *F. oxysporum* radial growth. Half growth inhibition was expressed as IC_{50} value derivate from the average of mycelial diameter treated with several extract concentrations. The IC_{50} of crude EA extract obtained from the W3.15 strain was recorded at 306.42 µg/ml according to regression of the dose-response curve (Figure 2). No growth reduction was found on the control plate. Meanwhile, the highest radial growth inhibition, with approximately 80%, was obtained from the highest final extract concentration (1,000 µg/ml).

3.4. Fungal Cell Damage by the Existence of Bacterial Extract

In vitro microscopical evaluation of bacterial extract supplementation on fungal culture medium was performed to confirm the hyphal response to extract. Compared with the typical hyphae, several hyphal alterations and cell damage were found on hyphae from the treated plate (Figure 3). The *F. oxysporum* started to develop alteration with globus formation along the hyphae as an effect of bacterial extract existence. The EA extract also induced the hyphae to grow abnormally; they turned twisted and curly (Figure 3). Chlamydospore (cl) was found on the hyphae with extract treatment and also enlargement of the vacuole (ev). Meanwhile, the changing that found in ketoconazole's treatment hyphae showed extensive twisted (th) and curly (ec) on fungal hyphae, along with excessive vacuolization (ev). In contrast, in this treatment was found some hyphal leakage (hl), marked with no blue pigmentation between hyphal septa that was not found on the extract treatment observation (Figure 3). Macro- and microconidia are rarely found on both treated plates and undergo shape deformation (not shown).

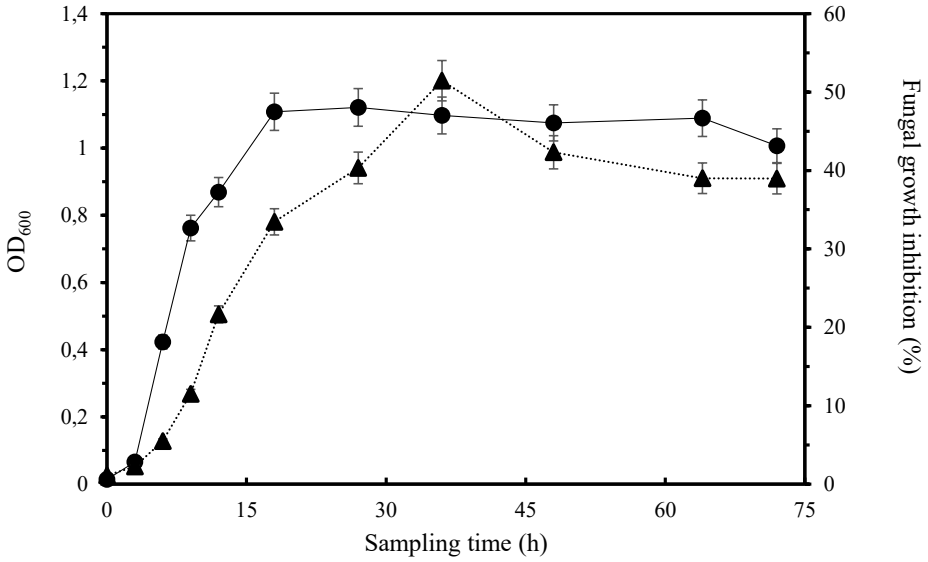

Figure 1. Correlation of *B. subtilis* strain W3.15 cell growth cultivated in NB basal medium for three days with its fungal inhibition activity. ▲ Indicates the antifungal activities of the CFS of strain W3.15 against *F. oxypsorum*. ● Means of the bacterial growth curve measured by OD_{600}

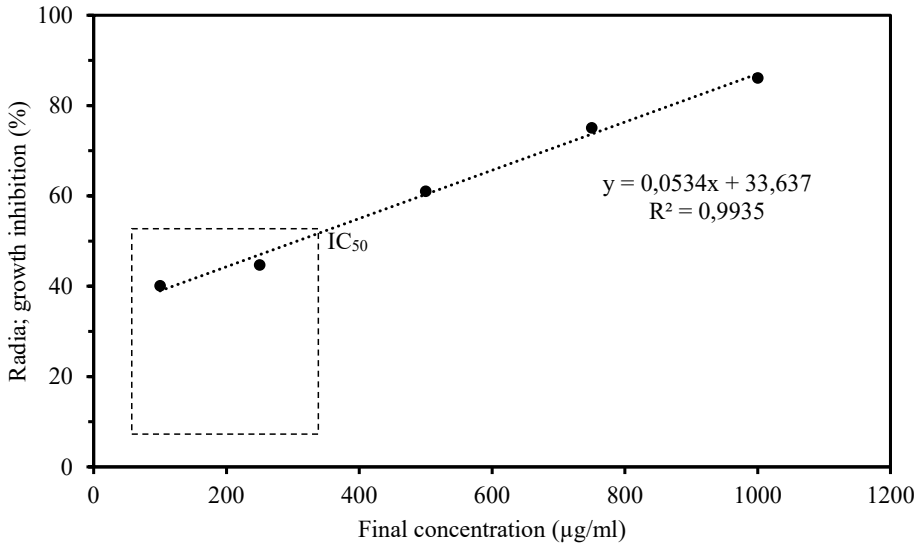

Figure 2. The dose-response regression curve of EA extract obtained from the strain W3.15 to determine the IC_{50} dosage for inhibiting radial growth of *F. oxysporum*

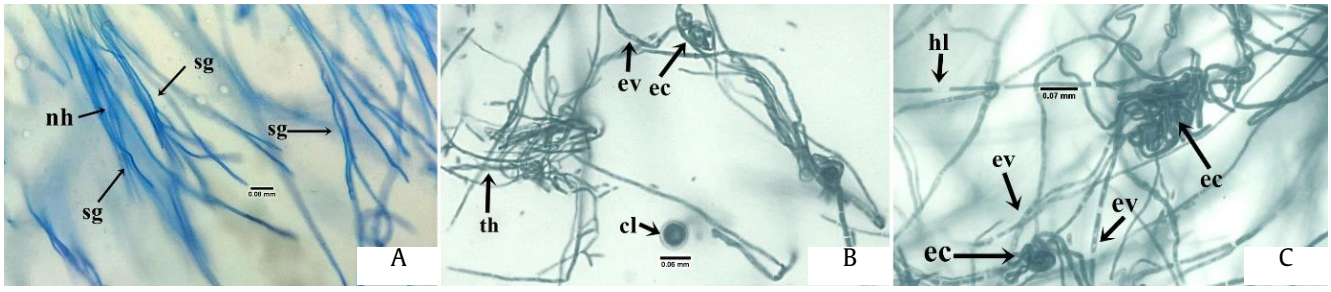

Figure 3. Light microscopic observations of crude EA extract of strain W3.15 deformation effect on hyphal morphology of *F. oxysporum* under 400x magnification: (A) untreated mycelium, (B) mycelium treated with IC_{50} dosage of crude EA, (C) mycelium treated with ketoconazole (500 µg/ml). nh: normal hyphae, sg: straight growth, cl: chlamydospore, hl: hyphal leakage, ev: enlargement of the vacuole, ec: excessively curly, and th: twisted growth of the hyphal. Bar 0.06 mm

3.5. The Effect of W3.15 Strain Crude EA Extract on Mycelial Malondialdehyde Content

The extent of damage in the lipid membrane of *F. oxysporum* mycelial after exposure to the IC_{50} concentration of crude EA extract was reflected by the malondialdehyde (MDA) level on fungal cells. As shown in Figure 4, the accumulation of MDA on the fungal cell was significantly ($p<0.05$) increased by the crude EA extract treatment after two days of incubation. The MDA level gradually increased and accumulated approximately 0.6 µmol/g mycelia on day three. The mycelial from the control tube also showed a significant increase ($p<0.05$) in MDA level during three days of incubation. However, the MDA level of control remains lower than that recorded in mycelia with bacterial extract treatment on each day of incubation. The maximum MDA accumulation on normal mycelia was recorded at 0.35 µmol/g mycelia on the second-day incubation before decreasing on the last day of incubation.

3.6. Impact of W3.15 Strain Crude EA Extract on Cell Membrane Leakage

Cell membrane leakage on *F. oxysporum* after exposure to bacterial extract was indicated by the release of intracellular content, such as protein and nucleic acid. The protein content of *F. oxysporum* that reflected by OD_{260} was showed gradually increased during incubation with the IC_{50} dosage. After three hours of incubation, the protein content of mycelia treated with IC_{50} dosage of the extract was significantly ($p<0.05$) higher than untreated mycelia (Figure 4). The maximum absorbance was recorded at 0.69 after four hours of incubation. A similar escalation pattern was shown on the absorbance at OD_{280} that reflects the nucleic acid leakage. The maximum absorbance was

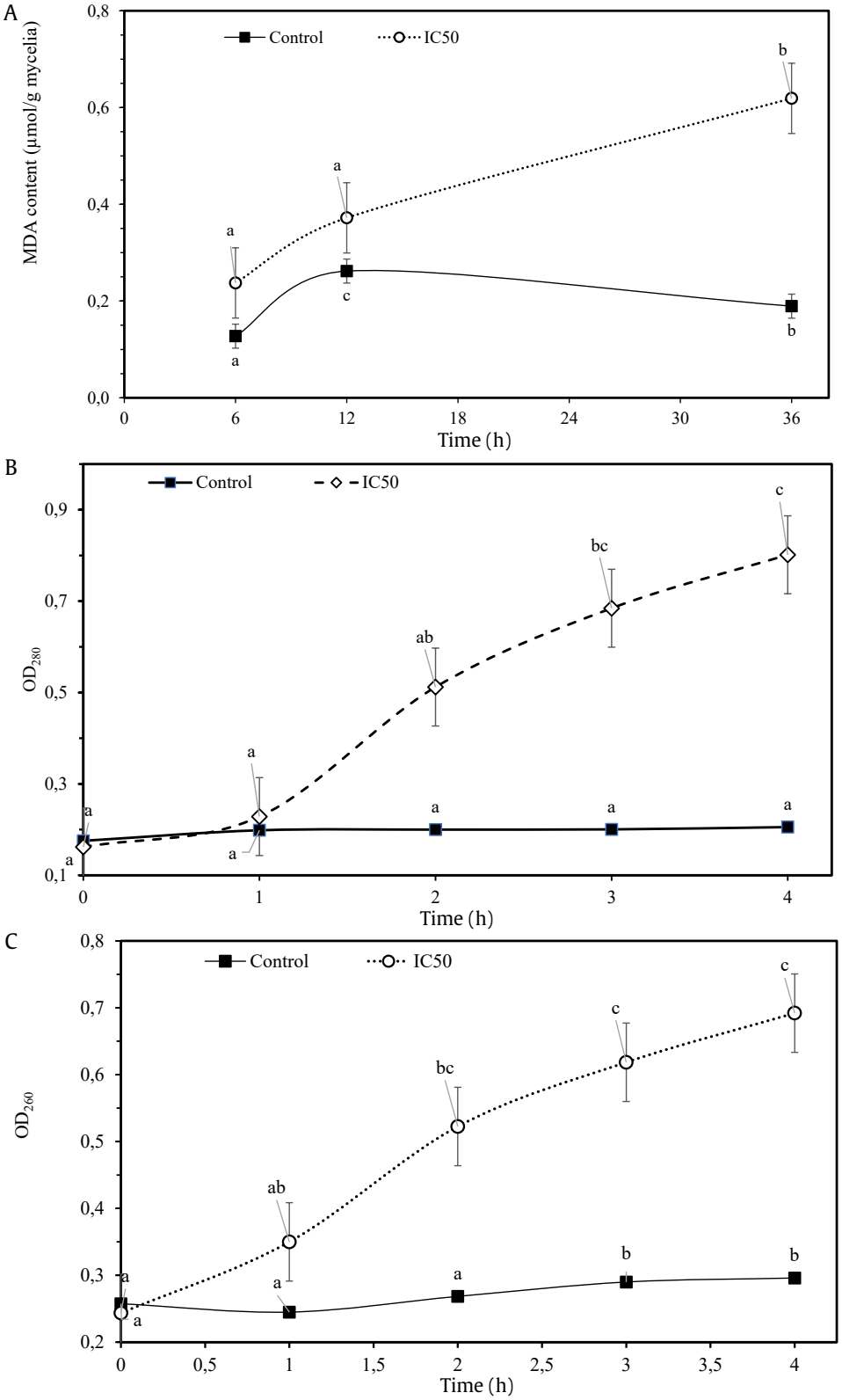

Figure 4. Effects of IC_{50} dosage of crude EA on *F. oxysporum* cell membrane permeability. (A) MDA level, (B) Protein leakage, (C) Nucleic acid leakage. Hyphae without extract supplementation were considered as the control of the experiment. The lowercase letters a, b, and c at the same time stamp indicate a significant difference at $p<0.05$

recorded at 0.80 and significantly higher than the absorbance of the control ($p<0.05$). The protein and nucleic acid absorbance of control mycelia did not significantly increase during incubation.

3.7. Predicted Antifungal Compounds of W3.15 Strain

Base peak ion (BPI) chromatogram of W3.15 crude EA extract achieved from LC-MS/MS analysis showed several dominant peaks along the retention times (0-22 min) (Figure 5). Four dominant peaks were detected respectively on 8.16 min, 9.12 min, and 10.07 min, and 10.71 min. Furthermore, two out of four dominant peaks were assumed to have antifungal compound spectra from the spectra and monoisotopic mass analysis on each peak. Proposed antifungal compounds, epicatechin (290.15 m/z) (Rt 10.71), diaveridine (260.17 m/z) (Rt 10.07), and benzophenone-8 (244.18 m/z) (Rt 9.11), were shared similar monoisotopic mass with the detected mass spectra of crude EA extract from W3.15 (Table 2). Meanwhile, the remaining dominant spectrum (Rt 8.15) was undefined due to unmatched mass spectra with the database. The peak of Rt 10.71 occupied 22.19% area, which was the highest value among others, followed by the second peak (Rt 10.07) as the second highest value, which occupied about 15.12% area.

4. Discussion

Different antimicrobial substances include cyclic lipopeptides (iturins, fengycins, and surfactins) produced by the Bacillus group (Ntushelo *et al.* 2019). Determining the appropriate culture medium for optimum secondary metabolite production with antifungal activity is necessary. Several types of common culture medium were used for W3.15 strain cultivation, which revealed that the NB basal medium remains the suitable cultivation medium for antifungal compound production. Though the NB medium showed lower biomass yield than the TSB medium, the latter medium has deficient antifungal activity expressed by a small value of the inhibition zone diameter. However, the TSB medium induced optimum cell growth for *Xenorhabdus stockie* PB09 with 70.73% fungal inhibition against phytopathogen *Phytophthora* sp. (Sa-Uth *et al.* 2018).

Additionally, the mung bean and egg yolk (MBE) medium was an important substrate for *B. amyloliquefaciens* PPL cell growth and biosurfactant production than the TSB medium as a common medium for the Bacillus group (Kang *et al.* 2020). The composition of medium and fermentation conditions influenced lipopeptide components' yield and synthesis.

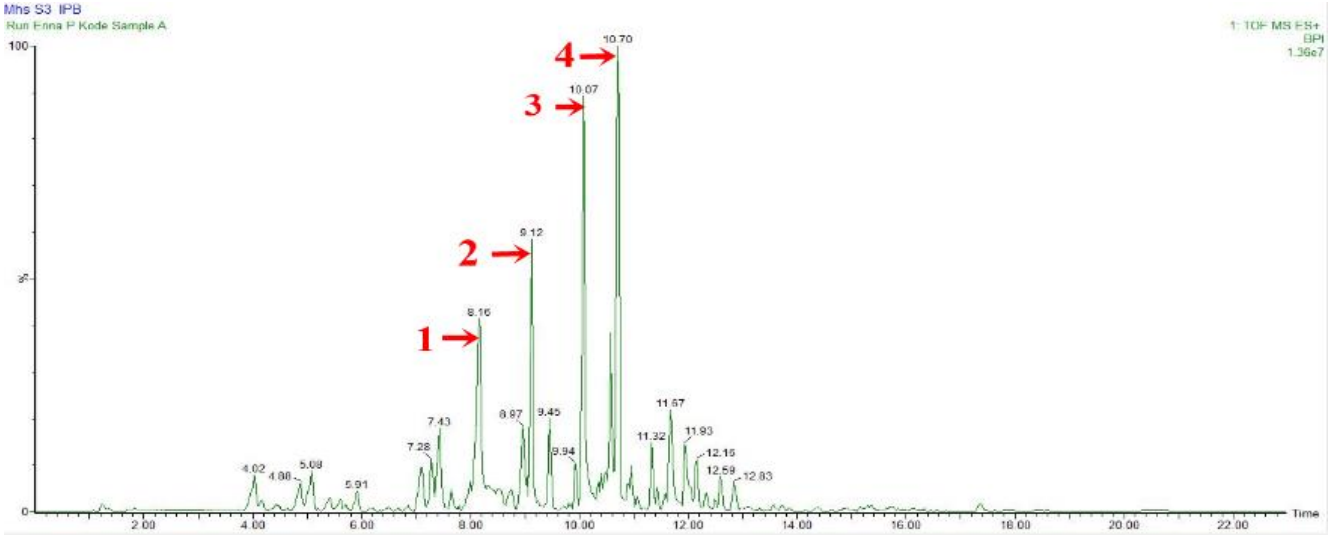

Figure 5. Base peak ion (BPI) chromatogram corresponding to LC-MS/MS analysis of the crude ethyl acetate extract generated from *B. subtilis* strain W3.15 shows four dominant peaks at 0-22 minutes of retention time

Thus, selecting the nutrient substrate for the maximum yield of antifungal lipopeptide (Kang *et al.* 2020; Medeot *et al.* 2017; Singh *et al.* 2014; Sun *et al.* 2019), especially for W3.15 strain was needed as a biocontrol agent for *F. oxysporum*.

In the NB medium, antifungal activity was detected in the logarithmic growth phase, progressively increasing and reaching the maximum inhibition towards *F. oxysporum* growth at the stationary phase. Rapid cell multiplication during the logarithmic phase indicated the higher synthesis of bacterial metabolite, then shifted to secondary metabolite at stationary, which induced high fungal inhibition in this phase (Rong *et al.* 2020). The antifungal compounds secreted by the W3.15 strain reached maximum concentration after the cell ceased and elicited high mycelial growth inhibition at this phase (36 h). A similar result was outlined by Li *et al.* (2018) regarding the secondary metabolite production of *B. tequilensis* GLYH001. *B. tequilensis* GLYH001 obtained the strongest antifungal activity against rice-blast pathogen *Magnaporthe oryzae* growth during the stationary phase 48 h post-inoculation. The cell growth of *B. amyloliquefaciens* Rdx5 also positively correlates with the antibiotic production that obtained the strongest inhibition to *M. oryzae* at the bacterial stationary phase (Dong *et al.* 2019). The optimal harvest time of *B. amyloliquefaciens* Rdx5 is two days post-inoculation cultured in a Landy medium (Dong *et al.* 2019). Hence, it assumed that secondary metabolites, including the antifungal compounds of the Bacilli group, were generally remarkably produced in the stationary phase from bacterial growth.

Regarding antifungal compound extraction, significant *in vitro* radial growth of *F. oxysporum* inhibition by crude EA extract indicated that several antifungal compounds were recovered through extraction. A higher extract concentration improved radial growth inhibition rates than the lowest concentration. According to Sukarno *et al.* (2021), there were three groups of inhibition in *F. oxysporum*, low inhibition (<30%), moderate inhibition (30-59%), and high inhibition (>60%), which confirmed that the inhibition of W3.15 strain extract was high. The previous report showed an impressive inhibition rate against three kinds of tuber dry rot pathogens, *F. acuminatum, F. equisetai*, and *F. tricintum*, by ethyl acetate extract of *Halobacillus trueperi* S61 (Shen *et al.* 2022). Those extracts showed the best suppression efficacy on *in vivo* potato tuber test. In addition, a strong antifungal effect against *F. graminearum* strain PH-1 *in vitro* and *in vivo* was shown by frenolicin B that recovered from the ethyl acetate extract of *Streptomyces* sp. NEAU-H3 supernatant (Han *et al.* 2021). Growth reduction in *F. oxysporum* implicated a disruption in cell metabolism during hyphal elongation, leading to substantial deformation after exposure to the bacterial extract.

Microstructural deformation and intracellular damage of mycelia exposed to bacterial extract were observed on *F. oxysporum* culture. As a comparison, swelling of hyphal cells, excessive branching, irregular growth, and suppressing conidiogenesis of *Magnaporthe oryzae* Triticum were evidence of gageopeptide A-D and gageotetrin produced by *B. subtilis* strain 109GGC020 treatment (Chakraborty *et al.* 2020). Severe irregularities and distortion of *F. verticillioides* mycelial showed in response to the treatment of Bacillomycin D purified from *B. subtilis* strain fmbJ (CGMCCN 0943) (Lin *et al.* 2022). Hence, the alterations of *F. oxysporum*, such as irregular and intensive twisted trunk growth on crude extract treatment plates, matched the result of those previous reports. The accumulation of various antifungal compounds in the crude EA extract seemed associated with the *Fusarium* growth suppression (Hwang *et al.* 2022) *F. oxysporum* mycelial growth undergoes intrusive action by the presence of antifungal substances from W3.15 strain, which induces oxidative stress on the fungal cell. Oxidative stress harms the intracellular, accumulates reactive oxygen species (ROS), and causes cell deterioration (Kulbacka *et al.* 2009).

The effect of ROS accumulation and cell damage occurred on fungal mycelial reflected by malondialdehyde (MDA) production (Dolezalova and Lukes 2015). Malondialdehyde is one of the most crucial products of membrane lipid peroxidation, indicating the damage degree of the membrane system (Dolezalova and Lukes 2015). The higher the degree of lipid peroxidation of the mycelial cell membrane, the higher the MDA content (Zhao *et al.* 2022b). Moreover, the MDA content in the mycelium of Sphaeropsis sapinea increased with exposure to extract from *B. pumilus* HR10-FB between 12 and 120 h (Dai *et al.* 2021). The result of this experiment confirmed some previous studies about the occurrence of oxidative stress in mycelia caused by bacterial extract application estimated by the MDA

level of the mycelial cell. Higher accumulation of MDA in the cell could damage the structure and function of the mycelial cell membrane altering the cell membrane conductivity and permeability (Dai *et al.* 2021). An increase in MDA accumulation suggests that cell membrane injury in *F. oxysporum* is related to the induction of oxidative damage by the bacterial extract. In contrast with the result above, the MDA content on *F. graminearum* treated with guaiacol was significantly lower compared to the control (Gao *et al.* 2021)

The consequence of high MDA exposure could destroy the cell membrane, followed by the release of nucleic acid, which showed strong absorption at 260 nm. On another side, as an important osmotic regulator, the accumulation of soluble proteins can improve the water retention capacity of cells, which protects the living substance and membrane of the fungal cell (Dai *et al.* 2021). Both nucleic acid and soluble proteins were essential materials for the growth and reproduction of cells, including fungal cell tip elongation. An increase in OD_{260} and OD_{280} on post-treated *F. oxysporum* with bacterial extract suggested that long-term exposure to extract accomplished membrane injury on *F. oxysporum* and led to cellular leakage. Cell membrane damage caused by iturin A from *B. subtilis* WL-2 on oomycete *P. infestans* was demonstrated by mycelium distortions and cellular leakage, including the increase of MDA level, absorbance on 260 nm (nucleic acids) and 280 nm (proteins) during 100 minutes incubation (Wang *et al.* 2020). However, a contrasting result was reported in olive fruit rot fungus *Pestalotiopsis microspore* treated with ginger oleoresin (EC_{50} and EC_{90}). The protein content in mycelia was not substantially affected by the concentration of the antifungal treatment during the incubation time (Chen *et al.* 2018). Thus, the cellular leakage might be influenced by the pathogen species or the antifungal substance treatment.

After determining the growth reduction effect and intracellular damage of *F. oxysporum* mycelia exposed to crude EA extract, antifungal compounds were identified through LC-MS/MS analysis. Predicted antifungal compounds were proposed from the analysis of epicatechin. The proposed antifungal compound was reported to show antifungal activity against damping-off fungi *Cylindrocarpon* sp. and *Colletotrichum dematium* and fruit rot fungus *Alternaria alternata* on cherry fruits (Wang *et al.* 2017; Yamaji and Ichihara 2012). The newest report related to the antifungal activity of epicatechin was the involvement of epicatechin as an important defensive compound against the tea tree pathogen *Ectropis grisescens* (Li *et al.* 2022). The other proposed compound was diaveridine which was reported as an antiprotozoal agent, while benzophenone was an antibacterial and antifungal compound (Jackson *et al.* 2015).

In this study, the authors finally successfully investigated the antifungal activity of *B. subtilis* strain W3.15 as a biocontrol agent for *F. oxysporum* that caused wilt disease in soybean, contributing to plant disease management strategy. Substantial radial growth reduction was obtained by organic solvent (EA) extract of supernatant W3.15 strain treatment *in vitro*. Growth reduction might be evidence of mycelial deformation and alternation triggered by active antifungal compounds. Furthermore, intracellular *F. oxysporum* cell response related to antifungal compounds was performed as malondialdehyde level and cellular leakage as a reflection of cell membrane damage. This study might help to ensure the mode of action of bacterial bioactive compounds in inhibiting fungal growth.

Acknowledgements

This research was funded by the Ministry of Education, Culture, Research, and Technology of the Republic of Indonesia, through the PMDSU scholarship (Grant number: 1/E1/KP.PTNBH/2021) for the 2018-2022 period.

References

Attia, M.S., Abdelaziz, A.M., Al-Askar, A.A., Arishi, A.A., Abdelhakim, A.M., Hashem, A.H., 2022. Plant growth-promoting fungi as biocontrol tool against *Fusarium* wilt disease of tomato plant. *J. Fungi.* 8, 775. https://doi.org/10.3390/jof8080775

Bhagat, N., Magotra, S., Gupta, R., Sharma, S., Verma, S., 2022. Invasion and colonization of pathogenic *Fusarium oxysporum* R1 in *Crocus sativus* L. during corm rot disease progression. *J. Fungi.* 8, 1246. https://doi.org/10.3390/jof812124

Bhar, A., Jain, A., Das, S., 2021. Soil pathogen, *Fusarium oxysporum* induced wilt disease in chickpea: a review on its dynamicity and possible control strategies. *Proc. Indian Natl. Sci. Acad.* 87, 260–274. https://doi.org/10.1007/s43538-021-00030-9

Chakraborty, M., Mahmud, N.U., Gupta, D.R., Tareq, F.S., Shin, H.J., Islam, T., 2020. Inhibitory effects of linear lipopeptides from a marine *Bacillus subtilis* on the wheat blast fungus *Magnaporthe oryzae triticum. Front. Microbiol.* 11, 665. https://doi.org/10.3389/FMICB.2020.00665/BIBTEX

Chen, T., Lu, J., Kang, B., Lin, M., Ding, L., Zhang, L., Chen, G., Chen, S., Lin, H., 2018. Antifungal activity and action mechanism of ginger oleoresin against *Pestalotiopsis microspora* isolated from chinese olive fruits. *Front. Microbiol*. 9, 1–9. https://doi.org/10.3389/fmicb.2018.02583

Cheung, N., Tian, L., Liu, X., Li, X., 2020. The destructive fungal pathogen Botrytis cinerea—insights from genes studied with mutant analysis. *Pathogens*. 9, 1–46. https://doi.org/10.3390/pathogens9110923

Dai, Y., Wu, X.Q., Wang, Y.H., Zhu, M.L., 2021. Biocontrol potential of *Bacillus pumilus* HR10 against *Sphaeropsis* shoot blight disease of pine. *Biol. Control*. 152, 104458. https://doi.org/10.1016/j.biocontrol.2020.104458

Derbyshire, M.C., Newman, T.E., Khentry, Y., Owolabi, T.A., 2022. The evolutionary and molecular features of the broad-host-range plant pathogen *Sclerotinia sclerotiorum. Mol Plant Pathol*. 23, 1075–1090. https://doi.org/10.1111/mpp.13221

Dimkić, I., Janakiev, T., Petrović, M., Degrassi, G., Fira, D., 2022. Plant-associated *Bacillus* and *Pseudomonas* antimicrobial activities in plant disease suppression via biological control mechanisms-a review. *Physiol. Mol. Plant Pathol.* 117, 101754. https://doi.org/10.1016/j.pmpp.2021.101754

Dolezalova, E., Lukes, P., 2015. Membrane damage and active but nonculturable state in liquid cultures of *Escherichia coli* treated with an atmospheric pressure plasma jet. *Bioelectrochemistry*. 103, 7–14. doi:10.1016/J.BIOELECHEM.2014.08.018

Dong, Y., Li, H., Rong, S., Xu, H., Guan, Y., Zhao, L., Chen, W., He, X., Gao, X., Chen, R., Li, L., Xu, Z., 2019. Isolation and evaluation of *Bacillus amyloliquefaciens* Rdx5 as a potential biocontrol agent against *Magnaporthe oryzae. Biotechnol. Biotechnol. Equip.* 33, 408–418. https://doi.org/10.1080/13102818.2019.1578692

Gao, T., Zhang, Y., Shi, J., Mohamed, S.R., Xu, J., Liu, X., 2021. The antioxidant guaiacol exerts fungicidal activity against fungal growth and deoxynivalenol production in *Fusarium graminearum. Front. Microbiol.* 12, 1–10. https://doi.org/10.3389/fmicb.2021.762844

Han, C., Liu, C., Xiang, W., Yu, Z., Zhang, Y., Wang, Z., Zhao, J., Huang, S.X., Ma, Z., Wen, Z., 2021. Discovery of frenolicin b as potential agrochemical fungicide for controlling *Fusarium* head blight on wheat. *J. Agric. Food Chem.* 69, 2108–2117. https://doi.org/10.1021/acs.jafc.0c04277

Han, D.S., Sheng, M.B., Zhu, M.D., Chen, D.J., Cai, D.H., Zhang, P.S., Guo, D.C., 2022. Role of FoERG3 in ergosterol biosynthesis by *Fusarium oxysporum* and the associated regulation by *Bacillus subtilis* HSY21 [In press]. *Plant Dis*. https://doi.org/10.1094/PDIS-05-22-1010-RE

Hwang, J.S., Song, H.G., 2020. Antifungal activity of *Bacillus subtilis* isolates against toxigenic fungi. K*orean J. Microbiol.* 56, 28–35. https://doi.org/10.7845/kjm.2020.0011

Hwang, S.H., Maung, C.E.H., Noh, J.S., Baek, W.S., Cho, J.Y., Kim, K.Y., 2022. Efficiency and mechanisms of action of pelletized compost loaded with *Bacillus velezensis* CE 100 for controlling tomato *Fusarium* wilt. *Biol. Control*. 176, 105088. https://doi.org/10.1016/j.biocontrol.2022.105088

Jackson, D.N., Yang, L., Wu, S.B., Kennelly, E.J., Lipke, P.N., 2015. *Garcinia xanthochymus* benzophenones promote hyphal apoptosis and potentiate activity of fluconazole against *Candida albicans* biofilms. *Antimicrob. Agents Chemother.* 59, 6032–6038. https://doi.org/10.1128/AAC.00820-15

Ji, Z., Liu, Y., Gao, R., Zhang, L., Zhu, F., Yang, L., Dong, J., Xu, J., 2022. Biocontrol potential of *Bacillus licheniformis* W10 against peach shoot blight caused by *Phomopsis amygdali [In press]. Eur. J. Plant Pathol.* https://doi.org/10.1007/s10658-022-02627-2

Jinal, H.N., Amaresan, N., 2020. Characterization of medicinal plant-associated biocontrol *Bacillus subtilis* (SSL2) by liquid chromatography-mass spectrometry and evaluation of compounds by *in silico* and *in vitro* methods. *J. Biomol. Struct. Dyn.* 38, 500–510. https://doi.org/10.1080/07391102.2019.1581091

Kang, B.R., Park, J.S., Jung, W.J., 2020. Antifungal evaluation of fengycin isoforms isolated from *Bacillus amyloliquefaciens* PPL against *Fusarium oxysporum* f. sp. lycopersici. *Microb. Pathog.* 149, 104509. https://doi.org/10.1016/j.micpath.2020.104509

Karlsson, I., Persson, P., Friberg, H., 2021. *Fusarium* head blight from a microbiome perspective. *Front. Microbiol.* 12, 1–17. https://doi.org/10.3389/fmicb.2021.628373

Kulbacka, J., Saczko, J., Chwilkowska, A., 2009. Oxidative stress in cells damage processes. *Pol. Merkur. Lekarski.* 27, 44–47.

Li, H., Guan, Y., Dong, Y., Zhao, L., Rong, S., Chen, W., Lv, M., Xu, H., Gao, X., Chen, R., Li, L., Xu, Z., 2018. Isolation and evaluation of endophytic *Bacillus tequilensis* GYLH001 with potential application for biological control of *Magnaporthe oryzae. PLoS One*. 13, 1–18. https://doi.org/10.1371/journal.pone.0203505

Li, W., Long, Y., Mo, F., Shu, R., Yin, X., Wu, X., Zhang, R., Zhang, Z., He, L., Chen, T., et al., 2021. Antifungal activity and biocontrol mechanism of *Fusicolla violacea* J-1 against soft rot in kiwifruit caused by *Alternaria alternata. J. Fungi*. 7, 937. https://doi.org/10.3390/jof7110937

Li, X., Zhang, J., Lin, S., Xing, Y., Zhang, X., Ye, M., Chang, Y., Guo, H., Sun, X., 2022. (+)-Catechin, epicatechin and epigallocatechin gallate are important inducible defensive compounds against *Ectropis grisescens* in tea plants. *Plant Cell Environ.* 45, 496–511. https://doi.org/10.1111/PCE.14216

Lin, F., Zhu, X., Sun, J., Meng, F., Lu, Z., Lu, Y., 2022. *Bacillomycin* D-C16 inhibits growth of *Fusarium verticillioides* and production of fumonisin B1 in maize kernels. *Pestic. Biochem. Physiol.* 181, 105015. https://doi.org/10.1016/j.pestbp.2021.105015.

Listyorini, K.I., Kusumaningrum, H.D., Lioe, H.N., 2021. Antifungal activity and major bioactive compounds of water extract of *Pangium edule* seed against *Aspergillus flavus. Int. J. Food Sci.* 2021, 1–10. https://doi.org/10.1155/2021/3028067

Liu, C., Sheng, J., Chen, L., Zheng, Y., Lee, D.Y.W., Yang, Y., Xu, M., Shen, L., 2015. Biocontrol activity of *Bacillus subtilis* isolated from *Agaricus bisporus* mushroom compost against pathogenic fungi. *J. Agric. Food Chem.* 63, 6009–6018. https://doi.org/10.1021/ACS.JAFC.5B02218

Medeot, D.B., Bertorello-Cuenca, M., Liaudat, J.P., Alvarez, F., Flores-Cáceres, M.L., Jofré, E., 2017. Improvement of biomass and cyclic lipopeptides production in *Bacillus amyloliquefaciens* MEP218 by modifying carbon and nitrogen sources and ratios of the culture media. *Biol. Control.* 115, 119–128. https://doi.org/10.1016/j.biocontrol.2017.10.002

Mejri, S., Siah, A., Coutte, F., Magnin-Robert, M., Randoux, B., Tisserant, B., Krier, F., Jacques, P., Reignault, P., Halama, P., 2018. Biocontrol of the wheat pathogen *Zymoseptoria tritici* using cyclic lipopeptides from *Bacillus subtilis. Environ. Sci. Pollut. Res.* 25, 29822–29833. https://doi.org/10.1007/s11356-017-9241-9

Miljaković, D., Marinković, J., Balešević-Tubić, S., 2020. The significance of *Bacillus* spp. in disease suppression and growth promotion of field and vegetable crops. *Microorganisms*. 8, 1–19. https://doi.org/10.3390/microorganisms8071037

Mohan, G., Thangappanpillai, A.K., Ramasamy, B., 2016. Antimicrobial activities of secondary metabolites and phylogenetic study of sponge endosymbiotic bacteria, *Bacillus* sp. at Agatti Island, Lakshadweep Archipelago. *Biotechnol. Reports*. 11, 44–52. https://doi.org/10.1016/j.btre.2016.06.001

Munakata, Y., Heuson, E., Daboudet, T., Deracinois, B., Duban, M., Hehn, A., Coutte, F., Slezack-deschaumes, S., 2022. Screening of antimicrobial activities and lipopeptide production of endophytic bacteria isolated from vetiver roots. *Microorganisms*. 10, 1–18. https://doi.org/10.3390/microorganisms10020209

Ntushelo, K., Ledwaba, L.K., Rauwane, M.E., Adebo, O.A., Njobeh, P.B., 2019. The mode of action of *Bacillus* species against *Fusarium graminearum*, tools for investigation, and future prospects. *Toxins (Basel)*. 11, 1–14. https://doi.org/10.3390/toxins11100606

Putri, R.E., Mubarik, N.R., Ambarsari, L., Wahyudi, A.T., 2021. Antagonistic activity of glucanolytic bacteria *Bacillus subtilis* W3.15 against *Fusarium oxysporum* and its enzyme characterization. *Biodiversitas J. Biol. Divers*. 22, 4067–4077. https://doi.org/10.13057/BIODIV/D220956

Qi, D., Zou, L., Zhou, D., Chen, Y., Gao, Z., Feng, R., Zhang, M., Li, K., Xie, J., Wang, W., 2019. Taxonomy and broad-spectrum antifungal activity of *Streptomyces* sp. SCA3-4 isolated from rhizosphere soil of *Opuntia stricta*. *Front. Microbiol*. 10, 1–15. https://doi.org/10.3389/fmicb.2019.01390

Rong, S., Xu, H., Li, L., Chen, R., Gao, X., Xu, Z., 2020. Antifungal activity of endophytic Bacillus safensis B21 and its potential application as a biopesticide to control rice blast. *Pestic. Biochem. Physiol*. 162, 69–77. https://doi.org/10.1016/j.pestbp.2019.09.003

Sa-Uth, C., Rattanasena, P., Chandrapatya, A., Bussaman, P., 2018. Modification of medium composition for enhancing the production of antifungal activity from *Xenorhabdus stockiae* PB09 by using response surface methodology. *Int. J. Microbiol*. 2018, 1-10. https://doi.org/10.1155/2018/3965851

Saxena, A.K., Kumar, M., Chakdar, H., Anuroopa, N., Bagyaraj, D.J., 2020. *Bacillus* species in soil as a natural resource for plant health and nutrition. *J. Appl. Microbiol.* 128, 1583–1594. https://doi.org/10.1155/2018/396585110.1111/jam.14506

Shen, S., Li, W., Wang, J., 2022. Inhibitory activity of *Halobacillus trueperi* S61 and its active extracts on potato dry rot. *Bioengineered.* 13, 3852–3867. https://doi.org/10.1080/21655979.2021.2024375

Singh, A.K., Rautela, R., Cameotra, S.S., 2014. Substrate dependent *in vitro* antifungal activity of *Bacillus* sp. strain AR2. *Microb. Cell Fact.* 13, 1–11. https://doi.org/10.1186/1475-2859-13-67

Srinivas, C., Nirmala, D.D., Narasimha, M.K., Mohan, C.D., Lakshmeesha, T.R., Singh, B.P., Kalagatur, N.K., Niranjana, S.R., Hashem, A., Alqarawi, A.A., Tabassum B., Abd_Allah E.F., Nayaka, S.C., Srivastava, R.K., 2019. *Fusarium oxysporum* f. sp. lycopersici causal agent of vascular wilt disease of tomato: biology to diversity-a review. *Saudi J. Biol. Sci*. 26, 1315–1324. https://doi.org/10.1016/j.sjbs.2019.06.002

Sukarno, N., Ginting, R.C.B., Widyastuti, U., Darusman, L.K., Kanaya, S., Batubara, I., Aryantha, I.N.P, Waite, M., 2021. Endophytic fungi from four Indonesian medicinal plants andtheir inhibitory effect on plant pathogenic *Fusarium oxysporum*. *HAYATI J. Biosci.* 28, 152–171. https://doi.org/10.4308/hjb.28.2.152

Sun, D., Liao, J., Sun, L., Wang, Y., Liu, Y., Deng, Q., Zhang, N., Xu, D., Fang, Z., Wang, W., Gooneratne, R., 2019. Effect of media and fermentation conditions on surfactin and iturin homologues produced by *Bacillus* natto NT-6: LC–MS analysis. *AMB Express*. 9, 120. https://doi.org/10.1186/s13568-019-0845-y

Sun, M., Ye, S., Xu, Z., Wan, L., Zhao, Y., 2021. Endophytic *Bacillus altitudinis* Q7 from Ginkgo biloba inhibits the growth of *Alternaria alternata in vitro* and its inhibition mode of action. *Biotechnol. Biotechnol. Equip*. 35, 880–894. https://doi.org/10.1080/13102818.2021.1936639

Veras, F.F., Correa, A.P.F., Welke, J.E., Brandelli, A., 2016. Inhibition of mycotoxin-producing fungi by *Bacillus* strains isolated from fish intestines. *Int. J. Food Microbiol.* 238, 23–32. https://doi.org/10.1016/j.ijfoodmicro.2016.08.035

Wan, Y., Zou, L., Zeng, L., Tong, H., Chen, Y., 2021. A new *Colletotrichum* species associated with brown blight disease on *Camellia sinensis*. *Plant Dis*. 105, 1474–1481. https://doi.org/10.1094/PDIS-09-20-1912-RE

Wang, M., Jiang, N., Wang, Y., Jiang, D., Feng, X., 2017. Characterization of phenolic compounds from early and late ripening sweet cherries and their antioxidant and antifungal activities. *J. Agric. Food Chem.* 65, 5413–5420. https://doi.org/10.1021/acs.jafc.7b01409

Wang, Y., Liu, X., Chen, T., Xu, Y., Tian, S., 2020. Antifungal effects of hinokitiol on development of *Botrytis cinerea in vitro* and *in vivo*. *Postharvest Biol. Technol*. 159, 111038. https://doi.org/10.1016/j.postharvbio.2019.111038

Wang Youyou, Zhang, C., Liang, J., Wu, L., Gao, W., Jiang, J., 2020. Iturin A extracted from *Bacillus subtilis* WL-2 affects *Phytophthora infestans* via cell structure disruption, oxidative stress, and energy supply dysfunction. *Front. Microbiol*. 11, 1–12. https://doi.org/10.3389/fmicb.2020.536083

Yamaji, K., Ichihara, Y., 2012. The role of catechin and epicatechin in chemical defense against damping-off fungi of current-year Fagus crenata seedlings in natural forest. *For. Pathol.* 42, 1–7. https://doi.org/10.1111/j.1439-0329.2010.00709.x

Zhao, H., Liu, K., Fan, Y., Cao, J., Li, H., Song, W., Liu, Y., Miao, M., 2022a. Cell-free supernatant of *Bacillus velezensis* suppresses mycelial growth and reduces virulence of *Botrytis cinerea* by inducing oxidative stress. *Front. Microbiol.* 13, 1–15. https://doi.org/10.3389/fmicb.2022.980022

Zhao, W.B., Zhao, Z.M., Ma, Y., Li, A.P., Zhang, Z.J., Hu, Y.M., Zhou, Y., Wang, R., Luo, X.F., Zhang, B.Q., Wang, Y.L., Hu, G.F., Liu, Y.Q., 2022b. Antifungal activity and preliminary mechanism of pristimerin against *Sclerotinia sclerotiorum*. *Ind. Crops Prod.* 185, 115124. https://doi.org/10.1016/j.indcrop.2022.115124